Available online at www.sciencedirect.com
ScienceDirect
Phytochemistry 68 (2007) 342–354
PHYTOCHEMISTRY
www.elsevier.com/locate/phytochem

Metabolic profiling and systematic identification of flavonoids and isoflavonoids in roots and cell suspension cultures of *Medicago truncatula* using HPLC–UV–ESI–MS and GC–MS

Mohamed A. Farag [a,b], David V. Huhman [a], Zhentian Lei [a], Lloyd W. Sumner [a,*]

[a] *Plant Biology Division, The Samuel Roberts Noble Foundation, P.O. Box 2180, Ardmore, OK 73401, USA*
[b] *Pharmacognosy Department, Faculty of Pharmacy, Kasr El Aini St., P.B. 11562, Cairo University, Egypt*

Received 1 March 2006; received in revised form 23 October 2006
Available online 6 December 2006

Abstract

An integrated approach utilizing HPLC–UV–ESI–MS and GC–MS was used for the large-scale and systematic identification of polyphenols in *Medicago truncatula* root and cell culture. Under optimized conditions, we were able to simultaneously quantify and identify 35 polyphenols including 26 isoflavones, 3 flavones, 2 flavanones, 2 aurones and a chalcone. All identifications were based upon UV spectra, mass spectral characteristics of protonated molecules, tandem mass spectral data, mass measurements obtained using a quadrupole time-of-flight mass spectrometer (QtofMS), and confirmed through the co-characterization of authentic compounds. In specific instances where the stereochemistry of sugar conjugates was uncertain, subsequent enzymatic hydrolysis of the conjugate followed by GC–MS was used to assign the sugar stereochemical configuration. Comparative metabolic profiling of *Medicago truncatula* root and cell cultures was then performed and revealed significant differences in the isoflavonoid composition of these two tissues.

Keywords: *Medicago truncatula*; Barrel medic; Leguminosae; Metabolic profiling; Isoflavonoids; High performance liquid chromatography (HPLC); Electrospray ionization (ESI); Gas chromatography (GC); Ion trap mass spectrometry (ITMS); Time-of-flight mass spectrometry (TOFMS)

1. Introduction

Legumes are important agricultural and commercial crops consumed in large quantities by both humans and animals. The Leguminosae taxonomic class includes a variety of plants with significant economic value including soybean, alfalfa, clover, pea, peanut, and various beans. Unfortunately, these economically important crops have large, polyploid genomes that are difficult to study at the molecular and genetic level. To overcome this obstacle, *Medicago truncatula*, a close relative of alfalfa, has been chosen as a model legume because of its small diploid genome (~5 × 108 bp), self-fertilization, genetically transformable, and prolific nature (Cook, 1999; Bell et al., 2000). Currently, we are utilizing *M. truncatula* cell suspension cultures originally generated from roots in a functional genomics project that incorporates profiling of gene expression (transcriptome), proteins (proteome), and metabolites (metabolome) to more completely interrogate and understand the integrated biological processes associated with legumes. As part of the metabolome approach, profiling of natural products such as saponins and phenolics is underway. Earlier, we reported on the metabolic profiling of saponins using HPLC coupled with ion trap mass spectrometry (ITMS; Huhman and Sumner, 2002) and this report focuses on phenolics.

Flavonoids are found throughout the plant kingdom, whereas isoflavonoids are more restricted and particularly prevalent in the Papilionoideae subfamily of the Leguminosae. These compounds function as preformed or inducible antimicrobial compounds, anti-insecticidal compounds, signaling molecules in symbiotic nodulation by *Rhizobium* bac-

* Corresponding author. Tel.: +1 580 224 6710; fax: +1 580 224 6692.
E-mail address: lwsumner@noble.org (L.W. Sumner).

0031-9422/$ - see front matter © 2006 Elsevier Ltd. All rights reserved.
doi:10.1016/j.phytochem.2006.10.023

teria, or as allelopathic agents (Dixon, 1999). Pterocarpan phytoalexins such as medicarpin and constitutive isoflavone malonyl glycosides are typical of the isoflavonoids from the medics (Dixon and Sumner, 2003). Dietary intake of isoflavonoids has a significant impact on both human and animal health based on their antimicrobial, estrogenic, antioxidant, or wide spectrum of other pharmacological activities (Rice-Evans et al., 1997).

Among the analysis methods used for flavonoids, the coupling of liquid chromatography (LC) with ultraviolet (UV) and/or electrospray ionization (ESI) mass spectrometric detection has been demonstrated as a powerful tool for the identification and quantification of phenolics in plant extracts (Niessen and Tinke, 1995). This approach has been used successfully in the identification of many isoflavonoids and their related glucoside and glucoside malonates in red and white clover (He et al., 1996; Lin et al., 2000; Klejdus et al., 2001, 2003; Wu et al., 2003). However, the configuration of attached sugars are often unconfirmed in most glycosides (Klejdus et al., 2001, 2003; Wu et al., 2003). Recently, UV absorbance combined with fluorescence detection (LC–UV–FLU) has been utilized in the structural elucidation of isoflavonoids in red clover (De Rijke et al., 2004).

This report presents a multiplexed approach utilizing HPLC–UV–ITMS and GC–MS for the profiling, systematic identification, and quantification of phenolics in roots and roots derived cell suspension cultures of *M. truncatula*. Data dependent tandem mass spectrometry (MS/MS) was performed to assist in the structural elucidation of both aglycones and glycosidic conjugates. Further, these MS based methods allowed us to differentiate, identify and quantitatively compare the phenolic compositions of *M. truncatula* roots and cell cultures.

2. Results and discussion

2.1. Analytical performance

HPLC–UV–MS was employed to qualitatively differentiate and identify the major flavonoid and isoflavonoid components present in *M. truncatula* suspension culture cells. Fig. 1 summarizes the flavonoid and isoflavonoid

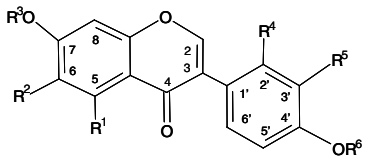

Isoflavone	R^1	R^2	R^3	R^4	R^5	R^6	M_r
Afrormosin	H	OCH_3	H	H	H	CH_3	298
Biochanin A	OH	H	H	H	H	CH_3	284
Daidzein	H	H	H	H	H	H	254
Formononetin	H	H	H	H	H	CH_3	268
2'-Hydroxyformononetin	H	H	H	OH	H	CH_3	284
Genistein	OH	H	H	H	H	H	270
Irilone	OH	-O-CH_2-		H	H	H	298
Irisolidone	OH	OCH_3	H	H	H	CH_3	314

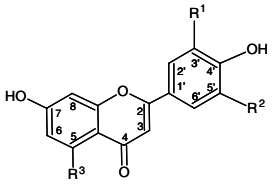

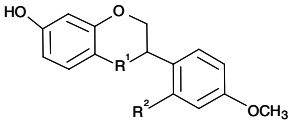

Flavone	R^1	R^2	R^3	M_r
7,4'-Dihydroxyflavone	H	H	H	254
5,3'-Dimethoxyluteolin	OCH_3	H	OCH_3	314
Tricin	OCH_3	OCH_3	OH	330

Pterocarpan/Isoflavan	R^1	R^2	M_r
Medicarpin	-CH-O-CH_2		270
Vestitol	CH_2	OH	286

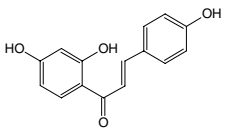

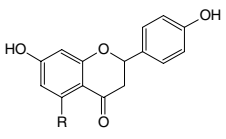

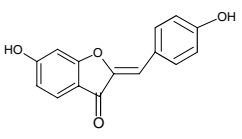

Chalcone	M_r
Isoliquiritigenin	256

Flavanone	R	M_r
Liquiritigenin	H	256
Naringenin	OH	270

Aurone	M_r
Hispidol	254

Fig. 1. Structures of identified aurone, chalcone, flavanone, flavone and isoflavone aglycones from *Medicago truncatula* root cell culture and root.

aglycones and conjugates observed in *M. truncatula* cell cultures. The method reported here is an adaptation of several previous methods developed and optimized for isoflavonoid profiling in *Trifolium* (clover), a close genus to *Medicago* (He et al., 1996; Lin et al., 2000; Klejdus et al., 2001, 2003; Wu et al., 2003). These earlier reports also provided significant structural and identity information concerning the isoflavonoid content in red and white clover based on mass and UV spectral data (Lin et al., 2000; Wu et al., 2003), and were found to be of great utility for analysis of *M. truncatula* roots and suspension culture cells. Unfortunately, HPLC–MS was not always able to determine the sugar linkage. In these situations, additional GC–MS following enzymatic hydrolysis and derivatization were applied to assist in identification of sugars and acylated moieties of isoflavonoid conjugates. For example, β-glucosidic linkage in glucose conjugates was confirmed by β-glucosidase treatment and the identity of the released sugar was determined by GC–MS relative to authentic reference compounds.

The reverse-phase HPLC–MS method reported here was similar to that previously reported (Wu et al., 2003); however the present method used slightly different mobile phases and a steeper gradient. In the present method, a steeper gradient of 0.1% aqueous acetic acid and acetonitrile was applied that allowed for the elution of all analytes within 70 min compared to the 100 min analysis time previously reported. Furthermore, the percentage of acetic acid was reduced from 0.25% to 0.1% resulting in a decrease in the mobile phase ionic strength and corresponding increase in signal to noise ratio as previously described for analysis of flavonoids in cocoa (Rabaneda et al., 2003). The elution order of the phenolics followed a sequence of decreasing polarity, whereby flavonoid diglucosides eluted first, followed by monoglucosides, acylated monoglucosides, and free aglycones. Simultaneously acquired HPLC–UV and HPLC–MS total ion chromatograms of *M. truncatula* cell culture extracts are presented in Fig. 2. The identities, retention times, characteristic observed molecular and fragment ions for individual components are presented in Table 1.

Photodiode array detection provided an overview of the main flavonoid constituents in *M. truncatula* suspension culture cells (Fig. 2A). UV spectra (200-600 nm) were recorded for different flavonoid sub-classes including 26 isoflavones (peaks **1–6**, **8**, **10**, **12**, **14**, **19–29** and **31–35**), 4 flavones (peaks **9**, **13**, **18** and **31**), 2 flavanones (peaks **21** and **30**), 2 aurones (peaks **7** and **11**) and a chalcone (peak **32**) with isoflavone representing the major sub-class. Each sub-class has a characteristic UV spectrum (Mabry et al., 1970). For example, isoflavones typically have a maximum absorbance near 255 nm with a second maximum between 300 and 330 nm (peak **34** in Fig. 2A), whereas aurones have the first maximum near 250 nm and the second peak around 390 nm (peak **7** in Fig. 2A). UV data were at or near literature values for those compounds previously described (Mabry et al., 1970; Wu et al., 2003); however, several compounds are reported here for the first time.

Extracts of *M. truncatula* suspension cell cultures derived from roots were analyzed in both the positive and negative-ion electrospray ionization (ESI) HPLC–MS modes to obtain a more comprehensive view of the phenolic content of suspension culture cells. Changes in ESI polarity can often circumvent or significantly alter competitive ionization and suppression effects revealing new metabolites (De Rijke et al., 2003). HPLC–MS files were further processed using AMDIS software to assist in adjacent peak deconvolution, background subtraction and lower detection limits (Halket et al., 1999). The positive-ion ESI mass spectra were characterized by cations corresponding to pseudo molecular species (i.e. $[M+H]^+$, $[M+K]^+$) and several lower m/z fragments ions attributed to the sequential loss of malonyl (86 amu) and hexosyl (162 amu) groups. These ions typically allowed for the determination of molecular weight, aglycone molecular weight, and the mass of sugar conjugates. From this data, the majority of the structures could be tentatively identified and then confirmed through the co-analysis of authentic standards. For example, peak **15** (R_t, 28.0 min) with a molecular ion at m/z 461 and a fragment ion of m/z 299 [461-glucosyl] in the MS spectrum (inset in Fig. 2B) was established as afrormosin 7-*O*-β-D-glucoside. Based on the above analyses, a total of 31 flavonoids, including 4 aglycones, 12 glucosides and 15 glucoside malonates were identified in *M. truncatula* cell culture. The elution order of flavonoids and their respective glucosides and glucoside malonates was similar to earlier reports conducted using RP-HPLC and acetonitrile elution (Lin et al., 2000; Wu et al., 2003).

The identification of the 31 flavonoids observed in positive-ion ESI mode were also validated using negative-ion ESI. Negative-ion, total ion chromatograms for suspension culture cells revealed better sensitivity and more observable peaks. The most notable improvements were for compounds eluting between R_t 35 and 40 min; i.e. the elution range of many aglycones (Fig. 2C). Additional peaks observed in the negative-ion ESI HPLC–MS and exhibiting a flavonoid-type UV spectra were identified as 7,4′-dihydroxyflavone (**18**), liquiritigenin (**21**), naringenin (**30**), tricin (**31**) and isoliquiritigenin (**32**). Additional peaks that did not exhibit a flavonoid-type UV spectra were detected, but were not examined further as part of this study. In contrast, 3 UV flavonoid peaks (**3**, **13** and **28**) were observed in positive-ion mode, but not detected in the negative-ion mode (Fig. 2C). Compared to the positive-ion ESI mode, negative-ion MS spectral characteristics were relatively simple with strong $[M-H]^-$ ions and very low abundance of fragment ions corresponding to sequential loss of sugar moieties. Lower fragmentation ion abundances (i.e. greater molecular ion abundances) and lower chemical noise resulted in higher signal-to-noise ratios for the molecular analyte species; and hence greater sensitivity. Negative-ion ESI HPLC–MS confirmed many of the glucoside molecular ions, however it did not yield as much fragmentation information as positive-ion. Thus, positive-ion pro-

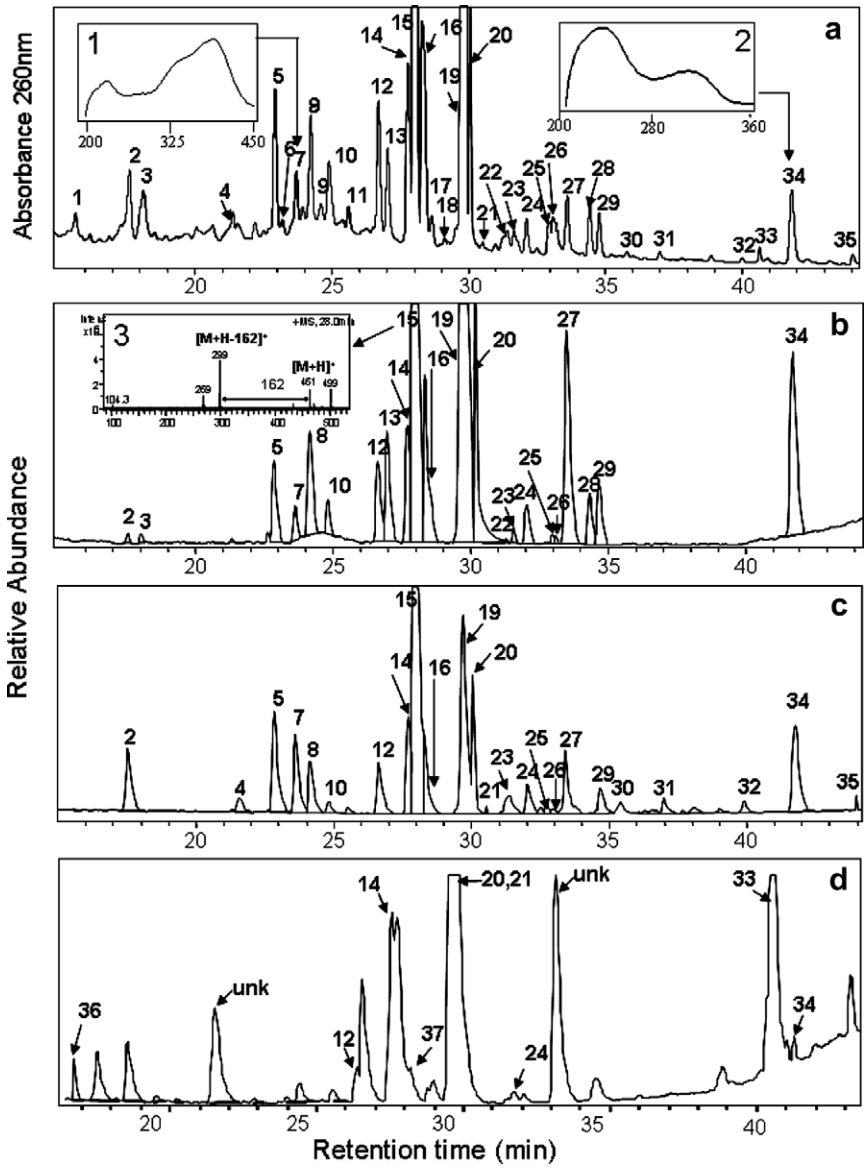

Fig. 2. HPLC–UV at 260 nm (A), HPLC–positive-ion ESI–MS (B), HPLC–negative-ion ESI–MS chromatogram of *M. truncatula* cell extracts (C), and HPLC–negative-ion ESI–MS chromatogram of *Medicago truncatula* roots (D), Insets 1 and 2 represents UV spectra of peak **7** (hispidol 4′-*O*-glucoside) and peak **34** (afrormosin), respectively, whereas 3 illustrates a full positive-ion MS spectra of peak **15** (afrormosin β-D-glucoside). Chromatographic conditions are described under Materials and Methods. The identities, R_t-value, UV and MS of all peaks are listed in Table 1.

vided more structural context and negative-ion greater sensitivity. It is interesting that the literature of legume isoflavonoids almost exclusively report positive ionization data (Barnes et al., 1994; He et al., 1996; Lin et al., 2000; Klejdus et al., 2001; Wu et al., 2003).

HPLC coupled to positive-ion ESI quadrupole time-of-flight mass spectrometry [(+)ESI–HPLC–QtofMS] was used to acquire improved mass accuracy data. Using this approach, mass accuracies in the range of 20–50 ppm were acquired compared with 2000 ppm obtained with the ion trap. The improved mass accuracy data are provided in Table 1 and significantly reduce the number of possible structures of putatively identified flavonoids. Additionally, the availability of an elaborate custom library of flavonoids (Mabry et al., 1970) allowed for the confirmation of all structures identified in cultured cells and in roots without ambiguity (Table 1).

2.2. Analysis of satellite sets

HPLC–MS metabolic profiling of the *M. truncatula* cell culture extracts revealed many glucoside and glucoside malonate conjugates with aglycones of same mass which are often referred to as satellite sets (De Rijke et al., 2004). To distinguish various satellite sets with the same aglycone mass, reconstructed ion chromatograms (RIC) were generated for each aglycone m/z observed in the TIC profile (upper trace, Fig. 3A). This process is valuable as it yields higher selectivity and sensitivity for structurally similar compounds as evidenced by more compounds

Table 1
Isoflavonoids identified by LC/ESI/UV/ITMS and LC/ESI/TOFMS in *Medicago truncatula* cell suspension culture extracts

Compound number	R_t (min)	Identification	Abbrev.	λ_{max} (nm)	Elemental composition	Qtof-MS $[M+H]^+$ m/z	HPLC–ITMS observed m/z(%) base peak	Identification procedure
1	15.8	Genistein β-D-di-glucoside	*GGG*	265, 328	$C_{27}H_{30}O_{15}$	595.6017	595(80)$[M+H]^+$; 433(100)$[M-Glc+H]^+$; 271(40) $[M-2Glc+H]^+$	b, d
2	17.6	Genistein β-D-di-glucoside-malonate	*GGGM*	259, 329	$C_{30}H_{32}O_{18}$	681.5002	681(100)$[M+H]^+$; 271(33)[M-malonyl-2Glc+H]$^+$	b, e
3	18.3	Daidzein 7-*O*-β-D-glucoside (daidzin)	*DG*	265, 310	$C_{21}H_{20}O_9$	417.3599	417(100)$[M+H]^+$; 255(36)$[M-Glc+H]^+$	a
4	21.1	Daidzein 7-*O*-β-D-glucoside-6″-*O*-malonate	*DGM*	258, 314	$C_{24}H_{12}O_{12}$	ND	503(100)$[M+H]^+$; 255(36)$[M-Glc+H]^+$	b, e
5	22.9	Biochanin A β-D-diglucoside	*BGG*	259, 316	$C_{28}H_{32}O_{15}$	609.5526	647(96)$[M+K]^+$; 609(100)$[M+H]^+$; 447(90)[M -Glc+H]$^+$; 285(16)$[M-2Glc+H]^+$	b, d
6	23.2	Genistein 7-*O*-β-D-glucoside (genistin)	*GG*	260, 325	$C_{21}H_{20}O_{10}$	433.4089	433(100)$[M+H]^+$; 271(46)$[M-Glc+H]^+$	a
7	23.4	Hispidol 4′-*O*-β-D- glucoside	*HG*	250, 350 sh, 395	$C_{21}H_{20}O_9$	417.1605	417(22)$[M+H]^+$; 255(100)$[M-Glc+H]^+$	a
8	24.2	Biochanin A β-D-diglucoside-malonate	*BGGM*	227, 260, 315	$C_{31}H_{34}O_{18}$	695.5975	695(100)$[M+H]^+$; 447(30)[M−malonyl-Glc+H]$^+$; 285(35)[M-malonyl-2Glc+H]$^+$	b, d
9	24.8	5,3′-Dimethoxyluteolin β-D-glucoside	*DLG*	258, 288, 335	$C_{23}H_{24}O_{11}$	477.4486	515(30)$[M+K]^+$; 477(40)$[M+H]^+$; 315(100)[M-Glc+H]$^+$	b, c, e
10	25.75	Genistein 7-*O*-β-D- glucoside-6″-*O*-malonate	*GGM*	265, 325	$C_{24}H_{22}O_{13}$	519.4567	519(100)$[M+H]^+$; 271(26)[M-malonyl-Glc+H]$^+$	b, d
11	25.65	Hispidol 4′-*O*-β-D- glucoside-malonate	*HGM*	252, 350sh, 397	$C_{24}H_{22}O_{12}$	503.1272	503(16)$[M+H]^+$; 255(100)[M-malonyl-Glc+H]$^+$	b, d
12	26.6	2′-Hydroxyformononetin β-D-glucoside	*HFG*	258, 325	$C_{22}H_{22}O_{10}$	447.4219	485(20)$[M+K]^+$; 447(26)$[M+H]^+$; 285(100)[M-Glc+H]$^+$	b, d
13	27.0	5,3′-Dimethoxyluteolin β-D-glucoside-malonate	*DLGM*	257, 287, 335	$C_{26}H_{26}O_{14}$	563.4897	563(100)$[M+H]^+$; 315(42)[M-malonyl-Glc+H]$^+$	b, c, e
14	27.5	Formononetin 7-*O*-β-D-glucoside (Ononin)	*FG*	252, 302	$C_{22}H_{22}O_9$	431.4222	469(30)$[M+K]^+$; 431(26)$[M+H]^+$; 269(100)[M-Glc+H]$^+$	a
15	28.0	Afrormosin 7-*O*-β-D-glucoside	*AG*	260, 321	$C_{23}H_{24}O_{10}$	461.4394	499(30)$[M+K]^+$; 461(26)$[M+H]^+$; 299(100)[M-Glc+H]$^+$	a
16	28.3	2′-Hydroxyformononetin β-D-glucoside-malonate	*HFGM*	258, 325	$C_{25}H_{24}O_{13}$	ND	533(36)$[M+H]^+$; 285(100)[M-malonyl-Glc+H]$^+$	b, e
17	28.4	Afrormosin 7-*O*-β-D-glucoside-malonate (isomer)	*AGM*	260, 325	$C_{26}H_{26}O_{13}$	547.4791	547(100)$[M+H]^+$; 299(100)[M-malonyl-Glc+H]$^+$	b, c , e
18	29.5	7,4′-Dihydroxyflavone	*DHF*	250sh, 322		ND	253(100)$[M-H]^-$	A
19	29.7	Afrormosin 7-*O*-β-D-glucoside-6″-*O*-malonate	*AGM*	228, 260, 321	$C_{26}H_{26}O_{13}$	547.4825	585(60)$[M+K]^+$; 547(100)$[M+H]^+$; 299(80)[M-malonyl-Glc+H]$^+$	b, c, d
20	29.8	Formononetin 7-*O*-β-D-glucoside-6″-*O*-malonate	*FGM*	250, 306	$C_{25}H_{24}O_{12}$	517.4535	517(35)$[M+H]^+$; 269(100)[M-malonyl-Glc+H]$^+$	a
21	30.4	Liquiritigenin	*L*	270, 315	$C_{15}H_{12}O_4$	257.2981	255(100)$[M-H]^-$	a
22	31.4	Vestitol β-D-glucoside-malonate	*VGM*	229, 282	$C_{25}H_{28}O_{12}$	521.2730	521(9)$[M+H]^+$; 273(11)[M-malonyl-Glc+H]$^+$	b, c

23	31.6	Irilone 4′-*O*-β-D-glucoside-6″-*O*-malonate	*IGM*	260, 325	$C_{25}H_{22}O_{14}$	ND	547(80)[M+H]$^+$; 299(100)[M-malonyl-Glc+H]$^+$	b, c, e
24	32.0	Medicarpin 3-*O*-β-D-glucoside	*MG*	233, 285	$C_{22}H_{24}O_9$	433.4738	471(100)[M +K]$^+$; 271(10)[M−Glc+H]$^+$	b, c, d
25	33.0	Irisolidone 7-*O*-β-D-glucoside	*SG*	265, 332	$C_{23}H_{24}O_{11}$	477.4471	515(29)[M+K]$^+$; 477(32)[M+H]$^+$; 315(100)[M−Glc+H]$^+$	b, e
26	33.1	Biochanin A 7-*O*-β-D-glucoside	*BG*	263, 322	$C_{22}H_{22}O_{10}$	447.4722	447(35)[M+H]$^+$; 285(100)[M−Glc+H]$^+$	a
27	33.5	Medicarpin 3-*O*-β-D-glucoside-malonate	*MGM*	230, 285	$C_{25}H_{26}O_{12}$	519.4780	557(100)[M+K]$^+$; 519(9)[M+H]$^+$; 271(15) [M-malonyl-Glc+H]$^+$	b, c, d
28	34.3	Irisolidone 7-*O*-β-D-glucoside-6″-*O*-malonate	*SGM*	265, 330	$C_{26}H_{26}O_{14}$	563.4931	601(35)[M+K]$^+$; 563(100)[M+H]$^+$; 315(38) [M-malonyl-Glc+H]$^+$	b, d
29	34.6	Biochanin A 7-*O*-β-D-glucoside-6″-*O*-malonate	*BGM*	260, 326	$C_{25}H_{24}O_{13}$	533.4484	571(20)[M+K]$^+$; 533(100)[M+H]$^+$; 285(25) [M-malonyl-Glc+H]$^+$	b, c, d
30	35.3	Naringenin	*N*	285, 330	$C_{15}H_{12}O_5$	ND	271 [M−H]$^-$	a
31	36.9	Tricin	*T*	ND	$C_{17}H_{14}O_7$	ND	329 [M−H]$^-$	a
32	40.0	Isoliquiritigenin	*I*	250, 300, 370	$C_{15}H_{12}O_4$	ND	255(100)[M−H]$^-$	a
33	40.7	Formononetin	*F*	250, 304	$C_{16}H_{12}O_4$	269.2534	269(100)[M+H]$^+$	a
34	41.6	Afrormosin	*A*	258, 320	$C_{17}H_{14}O_5$	299.3001	299(100)[M+H]$^+$	a
35	44.2	Medicarpin	*M*	230, 280	$C_{16}H_{14}O_4$	ND	269(100)[M−H]$^-$	a

Compounds are listed in order of elution from a C18 column and for simplification assigned the same numbering throughout the manuscript. Procedures employed for identification or tentative identification: a, co-analysis relative to a pure compound showing identical retention and mass data; b, comparison with literature MS and UV data; c, tandem MS/MS data of aglycone moiety; d, identification of enzymatically liberated aglycone and sugar moieties via HPLC–MS and GC–MS; e, identification of enzymatically liberated sugar moieties by GC–MS.

observed in the selected ion chromatograms than the UV or full scan MS mode. For example, the peaks in the extracted, positive-ion chromatogram for *m*/*z* 269 (Fig. 3B) commonly have a formononetin-based structure (*m*/*z* 269) and differ from each other in having a glucoside (**14**) or glucoside-malonate substituent (**20**). In the similar fashion, peaks in the RIC for *m*/*z* 285 (Fig. 3C) typically have biochanin A as their aglycone. These peaks were identified as biochanin A diglucoside BGG (peak **5**), biochanin A diglucoside-malonate BGGM (**8**), biochanin A glucoside BG (**26**) and biochanin A glucoside-malonate BGM (**29**). In legumes, many of the flavonoids occur as satellite sets of aglycones, glucosides, glucoside-malonates (Cook et al., 1995) and in some cases, glucoside acetates (Barnes et al., 1994). In the present study, six major "satellite sets" were found comprising 27 isoflavones, flavone glucosides and or glucoside malonates (Table 2). Moreover, satellite sets often revealed peaks that had the same mass, but different UV spectra as in case for 5,3′-dimethoxyluteolin (flavone) and irisolidone (isoflavone) glucosides (Table 2). Assignments of these peaks were based on the earlier elution of flavone glucoside (R_t 24.8) versus isoflavone glucoside (R_t 33.0) in addition to differences in their UV spectra (Table 2). Other spectral data including tandem MS were also used to differentiate between structural isomers in cases where UV and full scan mass data failed to confirm identification, as discussed in the next section.

2.3. Tandem mass spectrometry (MS–MS)

HPLC–UV analysis usually does not provide sufficient information necessary to distinguish between structural isomers such as the isoflavone afrormosin (λ_{max} 260, 321 nm) and irilone (λ_{max} 260, 325 nm). Increased structural information for afrormosin and/or irilone was obtained by tandem MS. Tandem MS was performed in a data dependent mode, isolating a molecular ion of interest (in this case the aglycone) followed by resonance excitation resulting in collisional activation and dissociation. The resulting fragment ions are directly related to the precursor ion and utilized in structural elucidation. One specific process involves the Retro-Diels-Alder (RDA) fragmentation of the aglycones with the same mass which yield different fragment ions that are observable during MS–MS analysis (Wu et al., 2003). For example, 5,3′-dimethoxyluteolin glucoside (peak **9**, R_t 24.8) and irisolidone glucoside (peak **25**, R_t 33.0) have the same molecular and fragment ions at *m*/*z* 477 and 315, respectively (Table 1). MS–MS analysis of precursor ions at *m*/*z* 315 in peak **9** and **25** showed a characteristic RDA fragment at *m*/*z* 167 and *m*/*z* 183 characteristic of 5,3′-dimethoxyluteolin and irisolidone, respectively. 5,3′-dimethoxyluteolin has been previously identified in alfalfa seeds as a nod gene-inducing flavonoid (Hartwig et al., 1990), however irisolidone has not been reported before in *Medicago*. Similarly, the glucoside malonates of afrormosin AGM (peak **19**, R_t 29.7) and irilone IGM (peak **23**,R_t 31.6) have similar UV

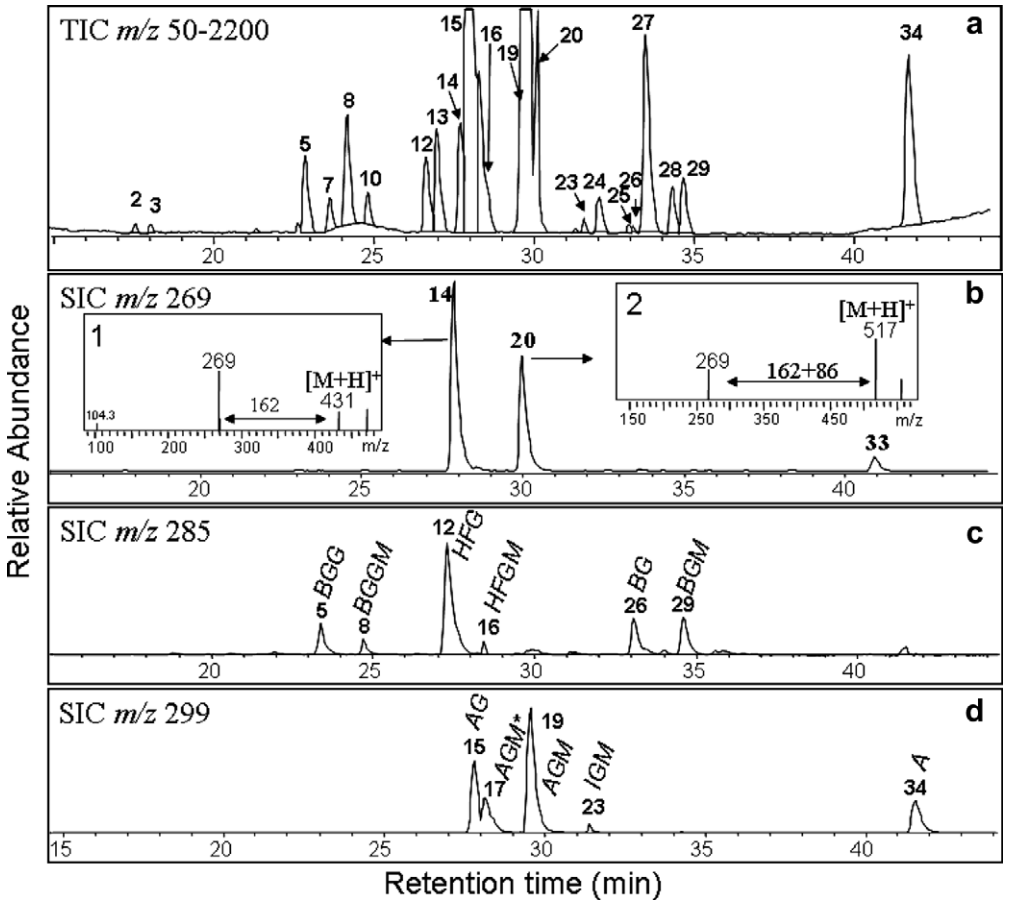

Fig. 3. Full scan (A), and selected positive-ion HPLC–ESI–MS chromatograms of *m/z* 269 (B), *m/z* 285 (C), and *m/z* 299 (D), of a *M. truncatula* cell culture extract. Panel B insets 1 and 2 provide mass spectra of peaks **14** (formononetin 7-*O*-β-D-glucoside) and peak **20** (formononetin 7-*O*-β-D-glucoside-malonate), respectively. See Table 1 for abbreviations.

Table 2
Polyphenol satellite sets observed in *M. truncatula* cell culture extracts

Flavonoid	λ_{max1} (nm)	λ_{max2} (nm)	Aglycone Mr	A	G	GM	GG	GGM
Hispidol	250	390	254		+	+		
Daidzein	258–265	305	254		+	+		
Formononetin	250	302–306	268	+	+	+		
Medicarpin	230–233	285	270		+	+		
Genistein	260	326	270		+	+	+	+
Biochanin A	260	315–320	284		+	+	+	+
2′-Hydroxyformononetin	258	325	284		+	+		
Afrormosin	255–260	320	298	+	+	+*		
Irilone	260	325	298			+		
Irisolidone	265	330-335	314		+	+		
5,3′-Dimethoxyluteolin	287	335	314		+	+		

+ presence detected, A – aglycone, G – glucoside, GM – glucoside malonate, GG – diglucoside, GGM – diglucoside malonate, * isomers observed.

spectra, same nominal molecular ions and characteristic $[M\text{-malonyl-glycosyl}+H]^+$ fragment ions at *m/z* 547 and 299, respectively (Table 1). However, these aglycones undergo different Retro-Diels-Alder (RDA) fragmentation yielding different fragment ions observable during MS–MS analysis. Further, the structures of medicarpin derivatives in peaks **24** (R_t 32.0) and **27** (R_t 33.5) were also confirmed from a characteristic RDA fragment at *m/z* 137 that coincided with standard medicarpin. Attempts to confirm aglycone structures at different activation energies did not always provide distinctive RDA fragment ions even though other additional fragmentation indicating loss of methyl groups were often observed. This was usually attributable to the lower concentration of these species that were insufficient to yield quality data for this acquisition mode. It is also worth mentioning that nega-

tive-ion ESI tandem MS of glycosidic conjugates typically did not reveal characteristic RDA fragment ions for the aglycones structures.

2.4. Malonate free extract analysis

The positive and negative-ion HPLC–MS analyses of *M. truncatula* cells revealed that malonated glucosides are the most abundant phenolic compounds compared to red clover in which glucosides were the most abundant as measured by peak area (Lin et al., 2000). Malonated glycosides are of biological interest in legumes because these conjugated forms are utilized to store the less soluble isoflavone aglycones, and upon microbial infection, the aglycones are liberated from the malonate conjugates (Edwards et al., 1997). While most isoflavonoid glucoside structures were confirmed using authentic chemical standards, malonated glucoside standards are not commercially available. However, malonated glucosides are thermally unstable and readily convert to their related glucosides upon heating by cleavage of the malonyl ester bond (Lin et al., 2000). This fact was exploited to confirm the structures of several glucoside malonates by comparative analysis of heated and unheated extracts. A total of seven major peaks identified as glucoside malonate conjugates were observed to shift to the corresponding glucoside after heat treatment. These included [BGGM(**8**) → BGG(**5**), DLGM(**13**) → DLG(**9**), HFGM(**16**) → HFG(**12**), AGM(**19**) → AG(**15**), FGM(**20**) → FG(**14**), MGM(**27**) → MG(**24**), and BGM(**29**) → BG(**26**)] as illustrated in Fig. 4. Both the malonated glucoside conjugates and related glucoside conjugates yielded highly similar UV spectra further supporting the structural identification and that the malonyl groups were directly attached to the sugar as opposed to the aglycone functional group which would result in UV spectral shifts (Mabry et al., 1970). These conclusions are also consistent with the structure of formononetin 7-*O*-β-D-glucoside 6″-*O*-malonate (peak **20**, R_t 29.8), which was established by comparison with authentic standard. Accordingly, other major malonated glucosides were assigned to have the same 6″-*O*-malonylglucosyl substitution pattern as that of the coexisting malonates and considering that they are most likely formed through a similar biogenetic pathway. This assignment is also supported by the fact that, so far, all of the flavonoid glucoside malonates from plants have a 6″-malonylglucosyl unit (Harborne, 1994; Lin et al., 2000).

It is worth mentioning that a minor peak (**17**) was detected of the same mass and UV spectra as that for afrormosin 7-*O*-β-D-glucoside 6″-*O*-malonate (**19**), Table 1. This minor malonate could possibly be an isomer of afrormosin 7-*O*-β-D-glucoside 6″-*O*-malonate in which the malonyl group was attached at a position other than 6″ at the glycosyl moiety. Alternative linkages between the malonyl and glucoside moieties have not been identified or reported for *Medicago*, however, glucoside malonate isomers of afrormosin, calycosin, formononetin and biochanin A have been detected in red and white clover (Lin et al., 2000; Edwards et al., 1997).

2.5. Identification of sugar and aglycone structures in flavonoid conjugates

Unfortunately, the absolute stereochemistry of the sugar constituents are not easily determined in phenolic

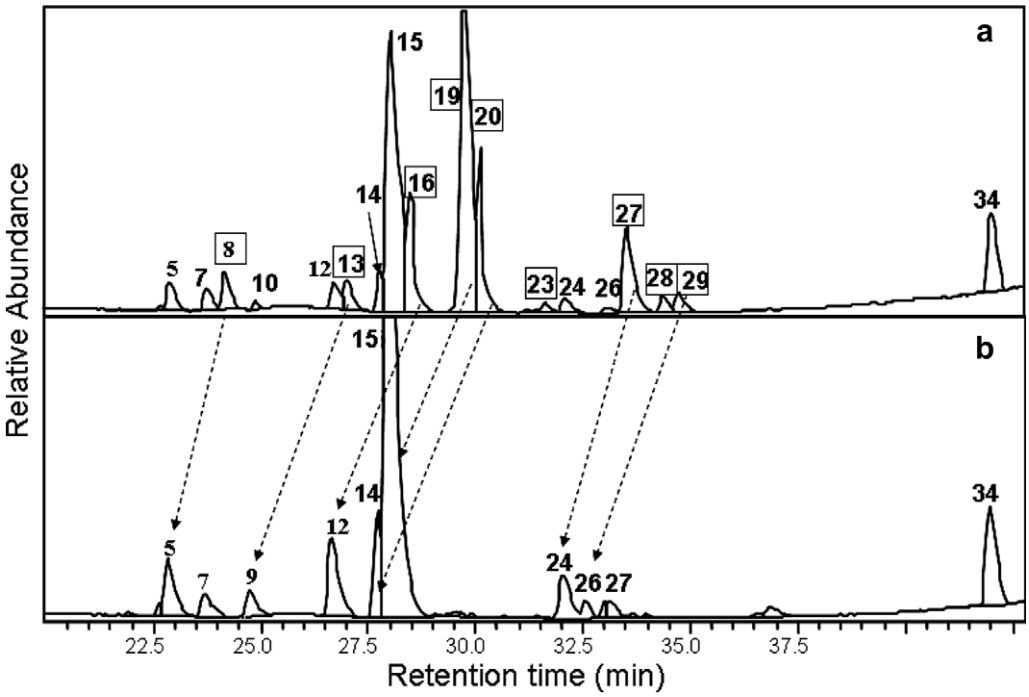

Fig. 4. Positive-ion HPLC–ESI–MS chromatogram of a *M. truncatula* cell culture extract (a), and a malonate free cell culture extract (b), following heat treatment. Boxed peak numbers represent malonated glucosides. Dashed arrows show conversion to corresponding glucosides following heating.

conjugates using HPLC–MS. For example, characteristic fragment ions can be readily classified as the loss of a hexose (162 amu), but it is much more difficult to confirm the sugar as glucose or galactose (Wu et al., 2003). To surmount this obstacle and to increase the confidence in our metabolite assignments, especially in cases where synthetic standards were unavailable, enzymatic hydrolysis and GC–MS was used to unambiguously characterize the aglycone and sugar constituents of each flavonoid. HPLC fractions corresponding to individual peaks were collected, hydrolyzed with β-glucosidase and the resulting sugar moieties were extracted, derivatized, and analyzed using GC–MS along side with authentic sugars. Glucose was identified as the only sugar moiety in all flavonoid and isoflavonoid conjugates; malonate was also detected in the GC–MS traces in case of malonated glucoside peaks. In clover and alfalfa, glucose was found to be the most common attached sugar in isoflavones (Lin et al., 2000; Klejdus et al., 2001, 2003). The anomeric configurations of the glucosidic linkages between aglycones and glucose moieties were established as β due to the specificity of the β-glucosidase used for all enzymatic hydrolysis experiments.

Positional attachment of the glucose groups were confirmed for afrormosin, biochanin A, daidzein, and formononetin glucosides to be on the 7 position of the aglycone by comparison with authentic standards. However glucose conjugation for irilone, irisolidone, 2′-hydroxyformononetin, genistein and 5,3′-dimethoxyluteolin could be at the 7, 2′, or 4′ positions of the aglycone and are still unconfirmed. Additionally, HPLC–UV–MS analysis of hydrolyzed glucosides were conducted to confirm the identity of the aglycone. The isoflavone aglycones afrormosin, daidzein, biochanin A, formononetin, 2′-hydroxyformononetin, and medicarpin were identified in their respective glucosides by comparison of the retention time, UV and mass spectral data with those of standard aglycones. Two novel diglucosides (peak **5**, R_t 22.9, m/z 609) and (peak **8**, R_t 24.2, m/z 695) were identified in the cell culture of *M. truncatula* (Table 1). The mass difference of 86 (amu) indicates an additional malonyl group in peak **8**. Both conjugates showed fragment ions corresponding to the consecutive loss of 2 glucose moieties (162 amu) and were identified as biochanin A β-D-diglucoside (**5**) and biochanin A β-D-diglucoside malonate (**8**). As expected, peak **8** disappears upon heating due the loss of malonate and conversion to its corresponding diglucoside (peak **5**; Fig. 4). The UV spectra for BGGM and BGG were almost identical to that of biochanin A 7-*O*-β-D-glucoside (BG) suggesting that both glucose moieties were attached at the same position in ring A (Mabry et al., 1970). However, the HPLC–UV–MS data could not unambiguously establish the interglycosidic linkage involved in both glucosides. To our knowledge, this is the first report of biochanin A β-D-diglucoside in both *Medicago* root and cell culture. Other diglucoside conjugates were detected and putatively identified as genistein-di-*O*-β-glucoside (**1**) and its malonylated conjugate (**2**); previously identified in *Lupinus hartwegii* aerial parts (Kamel, 2003).

2.6. Comparative analysis of flavonoids and isoflavonoids in *M. truncatula* suspension culture cells and roots

The *M. truncatula* suspension culture cells targeted in our functional genomics program and used here for profiling of isoflavonoids were originally derived from root tissue. Thus, qualitative and quantitative comparative analyses of culture cell and root phenolic content was performed to determine the impact of dedifferentiation and culturing on plant tissue. *M. truncatula* roots were extracted and analyzed under the same experimental conditions used for cell culture. Of the 35 phenolics identified in cell culture, only 17 were simultaneously found in roots with the conjugates of hispidol, irilone, irisolidone, genistein and 5,3′-dimethoxyluteolin not detected in roots (Table 3). On the other hand, two compounds assigned as 7,4′-dihydroxyflavone and isoliquiritigenin glucosides were detected in root, but not in cell culture. Relative quantitative analysis revealed that afrormosin conjugates AG and AGM were the major isoflavonoids in *M. truncatula* cell cultures, whereas formononetin conjugates FG and FGM predominate in *M. truncatula* roots. No significant differences were observed in vestitol or medicarpin glucoside content between root and cell extracts.

The *M. truncatula* cell culture composition data is consistent with previous reports citing AG and AGM as the major constitutive isoflavonoid present in alfalfa cell culture (Kessmann et al., 1990). These data support a high level of synergy between the model and crop legumes; however they also reveal significant differences between cell cultures and roots. A similar disparity has also been observed in alfalfa cell culture isoflavonoid profiles compared to roots (Tiller et al., 1994). This disparity is believed to be the result of induced genetic or epigenetic variation (Gould, 1987) during the culturing process and/or lack of differentiation in callus cells disrupting secondary metabolism regulatory networks (Jalal and Collin, 1977). For example, the most abundant isoflavones detected in cell culture were methylated at the 6 position of the A-ring (irilone, irisolidone, afrormosin) which suggests an increased activity of one or more *O*-methyltransferases (OMTs) in cell cultures relative to roots. The prerequisite for methylation is the presence of a hydroxyl group at the C-6 position. Currently, a flavonoid 6-hydroxylase (F6H) has not been characterized in *Medicago*, but a F6H has been characterized from soybean cell cultures (Latunde-Dada et al., 2001) supporting the presence of this enzyme in legumes. In addition, specific *Medicago* OMTs have not yet been characterized, but efforts in this area are underway (Deavours et al., 2006).

3. Conclusions

HPLC–UV–MS, HPLC–MS–MS, and GC–MS were used for metabolic profiling and systematic identification of flavonoids and isoflavonoids in roots and cell cultures of *M. truncatula*. The majority of structural information

Table 3
Comparison of flavonoid content of *Medicago truncatula* cell culture and root extracts

Compound number	R_t (min)	Assignment	Relative content in cell culture (*C*)	Relative content in root (*R*)	Ratio *C*/*R*
1	15.8	Genistein β-D-di-glucoside	0.06	ND	
2	17.6	Genistein β-D-di-glucoside-malonate	0.10	ND	
3	18.3	Daidzein 7-*O*-β-D-glucoside (Daidzin)	0.03	ND	
4	21.1	Daidzein 7-*O*-β-D-glucoside-6″-*O*-malonate (daidzin malonate)	0.03	ND	
5	22.9	Biochanin A β-D-di-glucoside	0.9[a]	0.02	45
6	23.2	Genistein 7-*O*-β-D-glucoside (genistin)	0.07	ND	
7	23.4	Hispidol 4′-*O*-β-D-glucoside	0.04	ND	
8	24.2	Biochanin A β-D-diglucoside-malonate	0.80	ND	
9	24.8	5,3′-Dimethoxyluteolin β-D-glucoside	0.2	ND	
10	25.75	Genistein 7-*O*-β-D-glucoside-6″-*O*-malonate	0.035	ND	
11	25.65	Hispidol 4′-*O*-β-D-glucoside-malonate	0.011	ND	
12	26.6	2′-Hydroxyformononetin β-D-glucoside	0.43[a]	0.03	14.5
13	27.0	5,3′-Dimethoxyluteolin β-D-glucoside-malonate	0.27	ND	
14	27.5	Formononetin 7-*O*-β-D-glucoside (Ononin)	0.6	0.4	1.65
15	28.0	Afrormosin 7-*O*-β-D-glucoside	2.8[a]	0.03	95
16	28.3	2′-Hydroxyformononetin β-D-glucoside-malonate	0.9	ND	
17	28.4	Afrormosin 7-*O*-β-D-glucoside-malonate (isomer)	2.8[a]	0.07	40
18	29.5	7,4′-Dihydroxyflavone	0.05	0.08	0.6
19	29.7	Afrormosin 7-*O*-β-D-glucoside-6″-*O*-malonate	3.0[a]	0.07	42
20	29.8	Formononetin 7-*O*-β-D-glucoside-6″-*O*-malonate	0.2[a]	1.1	0.18
21	30.4	Liquiritigenin	0.03	0.18	0.16
22	31.4	Vestitol β-D-glucoside-malonate	0.12	0.07	1.7
23	31.6	Irilone 4′-*O*-β-D-glucoside-6″-*O*-malonate	0.07	ND	
24	32.0	Medicarpin 3-*O*-β-D-glucoside	0.28	0.15	1.9
25	33.0	Irisolidone 7-*O*-β-D-glucoside	0.10	ND	
26	33.1	Biochanin A 7-*O*-β-D-glucoside	0.08	ND	
27	33.5	Medicarpin 3-*O*-β-D-glucoside-malonate	0.30	0.6	0.5
28	34.3	Irisolidone 7-*O*-β-D-glucoside-6″-*O*-malonate	0.09	ND	
29	34.6	Biochanin A 7-*O*-β-D-glucoside-6″-*O*-malonate	0.16	ND	
30	35.3	Naringenin	0.004	ND	
31	36.9	Tricin	0.03	0.06	0.5
32	40.0	Isoliquiritigenin	0.05	0.13	0.4
33	40.7	Formononetin	0.04[a]	0.6	0.06
34	41.6	Afrormosin	0.25[a]	0.03	8.5
35	44.2	Medicarpin	0.004[a]	0.03	0.15
36	17.4	7,4′-Dihydroxyflavone β-D-glucoside	ND	0.04	
37	28.5	Isoliquiritigenin 4′-*O*-β-D-glucoside	ND	0.25	

Note that compounds number **36** and **37** are not included in Table 1 and were only identified in roots.
Values are expressed as relative peak areas normalized to the recovered amount of umbelliferone added as an internal standard.
[a] Values followed by letter within the same row are significantly different. ND not detected.

was derived from full-scan and extracted positive-ion ESI–MS, which yielded characteristic fragmentation patterns of aglycones, the presence of sugar moieties and malonate groups. Tandem MS provided additional information allowing the structural confirmation of many aglycones based on Retro-Diels-Alder fragment ions. Sugar linkage and identification was confirmed using GC–MS following enzymatic hydrolysis and derivatization. Using the multiple optimized HPLC and MS conditions, 35 polyphenols were identified from *M. truncatula* cell culture including 12 glucosides, 15 glucoside malonates and 8 free aglycones. Our results also demonstrate that there are significant quantitative and qualitative differences in the isoflavonoid compositions of root and cell cultures derived from same tissue, a common situation in cell cultures (Jalal and Collin, 1977; Gould, 1987; Tiller et al., 1994).

To the best of our knowledge, this is the first, in-depth metabolic profiling study of phenolics in *M. truncatula*, a model organism for plant and legume genomic research. The identified phenylpropanoids provide a more complete atlas of the chalcone, aurone, flavone and isoflavone biosynthetic networks in *M. truncatula*. These metabolic atlases are beginning to yield insight into the functional annotation of biosynthetic enzymes such as *O*-methyltransferases (Deavours et al., 2006). These detailed metabolic maps will also facilitate more efficient metabolic engineering efforts to improve the composition of these health promoting phytochemicals and future improvements in the major forage crop alfalfa. Further, these data provide a foundation for comparative metabolic profiling of isoflavonoids in the context of a broader functional genomics program in *M. truncatula.*

4. Experimental

4.1. Materials

4.1.1. Biological materials

Liquid suspension cell cultures were derived from *Medicago truncatula* cv Jemalong A17 roots, grown in the dark in 500 ml shaker flasks, and suspended in Schenkand Hildebrandt (SH) medium with transfer to fresh medium every 2 weeks. Cells were harvested 4 d after transfer while in log-phase growth, washed once with fresh SH medium and once with SH:water (1:1 [v/v]), ground in liquid N_2 and immediately lyophilized. Plant root tissue was collected from 6 weeks old seedlings grown in Turface MVP™ (Profile Products, Buffalo Grove, IL) medium. Seedlings were grown in a controlled greenhouse environment maintained at an average temperature of 28 °C, 40% humidity, and a daylight period of 16 h.

4.1.2. Chemicals

Biochanin A, sissotrin, ononin, daidzin, daidzein, formononetin, 7,4′-dihydroxyflavone and prunetin were purchased from Indofine (Somerville, NJ, USA); hispidol, vestitol, afrormosin and afrormosin glucoside from Apin Chemicals Limited (Abingdon, UK). 2′-hydroxyformononetin, formononetin glucoside malonate and medicarpin glucosides and glucoside malonates were isolated and purified from alfalfa. Irisolidone, hispidol 4′-*O*-glucoside and tricin were kindly provided by Prof. Tom Mabry (University of Texas at Austin, TX, USA). Isoliquiritigenin, liquiritigenin and naringenin were purchased from Sigma-Aldrich (St. Louis, MO). All solvents used were HPLC–MS or GC–MS grade.

4.1.3. Extraction

Lyophilized *M. truncatula* suspension culture cells or root tissue (20 ± 0.06 mg) were extracted with 1.8 ml aq. 80% MeOH for 10 h using an orbital shaker in the dark. Extracts were centrifuged at 3000*g* for 60 min and 1.4 ml of the supernatant was removed and evaporated under nitrogen till dryness. The dried residue was resuspended in 300 μl of 45% aq. MeOH. For comparative analysis, the extracts were spiked with 2 μg umbelliferone as an internal standard (IS) and relative quantifications determined based on HPLC–MS peak areas that were normalized based on the area of the recovered IS peak.

4.1.4. Hydrolysis of malonated conjugates

M. truncatula extracts resolubilized in 45% aq. MeOH were heated in a sealed vial at 80 °C for 16 h and then left at room temp. for 1 h. This process converts flavonoid glucoside malonates to their glucosides without the production of other derivatives (Lin et al., 2000).

4.1.5. Hydrolysis and analysis of sugar and aglycone constituents

M. truncatula extracts resolubilized in 45% MeOH in water were separated using HPLC and the same conditions used for analysis described below in the LC–ESI–MS Instrumentation section, except the flow rate was lowered to 0.5 ml min^{-1}. The instrumental response of the PDA was monitored at 260 nm and targeted peaks/fractions collected. Collected fractions were evaporated, re-suspended in 200 μl water, heated as mentioned above to cleave malonyl conjugates, and subjected to hydrolysis using β-glucosidase (Mabry et al., 1970) for 8 h at 37 °C. The aglycones were then partitioned from the aqueous phase into EtOAc (3×2 ml). The EtOAc fractions were evaporated to dryness under nitrogen, residues re-suspended in 100 μl MeOH, and analyzed using HPLC–UV–MS to characterize target aglycones. The aqueous phase following liquid–liquid extraction with EtOAc and containing the liberated sugars was evaporated in a SpeedVac to complete dryness. The sugars were derivatized as described below and analyzed by GC–MS in parallel with authentic sugars, e.g. glucose, galactose and malonic acid.

4.1.6. Sugar derivatization

Sugars were methoximated and trimethylsilylated (TMSi) to improve chromatographic behavior using stan-

dard methods in our lab (Broeckling et al., 2005). 70 μl of 15 mg ml^{-1} methoxyamine hydrochloride in pyridine was added and incubated at 50 °C for 60 min, followed by 30 μl of *N*-methyl-*N*-trimethylsilyltrifluoroacetamide (MSTFA) + 1% trimethylchlorosilane (TMCS) (Pierce, Rockford, IL) in pyridine and incubated at 50 °C for 30 min. TMSi-sugars were analyzed using GC–MS and identified based on GC–MS retention time and spectral characteristics of authentic derivatized sugars, e.g. glucose, galactose and malonic acid.

4.2. HPLC–ESI–MS instrumentation

An Agilent 1100 series II HPLC system (Hewlett-Packard, Palo Alto, CA) equipped with a photodiode array detector was coupled to a Bruker Esquire ion-trap mass spectrometer via an electrospray ionization (ESI) source. UV spectra were obtained by scanning from 200 to 600 nm. A reverse phase, C18, 5 μm, 4.6 × 250 mm column (J.T.Baker, Phillipsburg, NJ) and a linear gradient of 5–90% B (v/v) over 70 min were utilized for separations. The mobile phases consisted of eluent A (0.1% aq. HOAc) and eluent B (acetonitrile). The flow rate was 0.8 ml min^{-1} and the temperature of the column was maintained at 28 °C. Both positive and negative-ion ESI mass spectra were acquired. Positive-ion ESI was performed using an ion source voltage of 4.0 kV and a capillary offset voltage of 86.0 V. Nebulization was aided with a coaxial nitrogen sheath gas provided at a pressure of 60 psi. Desolvation was assisted using a counter current nitrogen flow set at a pressure of 12 psi. and a capillary temperature of 300 °C. Mass spectra were recorded over the range 50–2200 *m*/*z*. The Bruker ion-trap mass spectrometer (ITMS) was operated using an ion current control (ICC) of approximately 10,000 with a maximum acquire time of 100 ms. Tandem mass spectra were obtained in manual mode for targeted masses using an isolation width of 2.0, fragmentation amplitude of 2.2 and threshold set at 6000. HPLC–MS data files were analyzed using AMDIS (Automated Mass Spectral Deconvolution and Identification System) available at http://chemdata.nist.gov/mass-spc/amdis.

4.3. HPLC–QtofMS instrumentation

Positive-ion HPLC–ESI–Qtof mass spectra were recorded on an ABI QSTAR Pulsar *i* hybrid quadrupole time-of-flight mass spectrometer (QtofMS; Applied Biosystems, Framingham, MA) coupled with an Agilent 1100 series II HPLC system (Hewlett-Packard, Palo Alto, CA). Ionization was achieved using a turbo-ion electrospray source voltage of 5.5 kV with N_2 as the nebulizer gas. The QtofMS was operated in the wide-pass quadrupole mode between *m*/*z* 50 and 850 and with a low collision energy of 25 eV to ensure integrity of the molecular species. All analyses were acquired using an independent reference lock-mass ion to ensure accuracy and reproducibility. Commercially obtained ononin (*m*/*z* 430.1081) and afrormosin (*m*/*z* 298.0720) were used as reference compounds, injected either separately or in a mixture and analyzed under the same conditions. HPLC separation was achieved using a reverse phase, C18, 5 μm, 4.6 × 250 mm column (J.T.Baker, Phillipsburg, NJ) and a liner gradient from 90% eluent A (0.1% aq. HOAc) and 10% eluent B (acetonitrile) to 90% eluent B over 70 min at a flow rate of 0.3 ml min^{-1}.

4.4. GC–MS instrumentation

An HP 6890 GC (Hewlett-Packard, Palo Alto, CA) equipped with a 60 m DB-5-MS column (J&W Scientific, 0.25 mm ID, 0.25 μm film thickness) was coupled to an HP 5973 quadrupole mass spectrometer. Samples were injected in a split mode using a split ratio of 1:1, an inlet and transfer line temperature of 250 °C, and a constant He flow of 1.0 ml min^{-1}. Separation was achieved with a temperature program with an initial temperature of 80 °C and initial time of 2 min which was then ramped to 315 °C at 5 °C min^{-1} and held at 315 °C for 12 min. The MS source was maintained at 250 °C and the quadrupole at 150 °C. Mass spectra were recorded while scanning from 50–650 *m*/*z* following optimization of MS parameters and mass calibrations using the manufacturers autotune macro.

Acknowledgements

The authors thank Dr. Qingli Wu, Department of Plant Biology and Pathology, Rutgers University for providing irilone from red clover, and Dr. Bettina Deavours, Samuel Roberts Noble Foundation, for helpful discussions and manuscript review. This project was financially supported by The National Science Foundation Plant Genome Research Program Award #DBI-0109732 and The Samuel Roberts Noble Foundation.

References

Barnes, S., Kink, M., Coward, L., 1994. Isoflavones and their conjugates in soy foods; extraction and analysis by HPLC–mass spectrometry. J. Agric. Food Chem. 42, 2466–2474.

Bell, C.A., Dixon, R.A., Farmer, A.D., Flores, R., Inman, J., Gonzales, R.A., Harrison, M.J., Paiva, N.L., Scott, A.D., Weller, J.W., May, G.D., 2000. The *Medicago* genome initiative: a model legume database. Nucl. Acids Res. 29, 1–4.

Broeckling, C.D., Huhman, D.V., Farag, M., Smith, J.T., May, G.D., Mendes, P., Dixon, R.A., Sumner, L.W., 2005. Metabolic profiling of *Medicago truncatula* cell cultures reveals effects of biotic and abiotic elicitors on metabolism. J. Exp. Bot. 56, 323–336.

Cook, R., Tiller, S.A., Mizen, K.A., Edwards, R., 1995. Isoflavonoid metabolism in resistant and susceptible cultivars in white clover infected with the stem nematode *Ditylenchus dipsaci*. J. Plant Physiol. 146, 348–354.

Cook, D.R., 1999. *Medicago truncatula* – a model in the making! Curr. Opin. Plant Biol. 2, 301–304.

De Rijke, E., Zappey, H., Ariese, F., Gooijer, C., Brinkman, U.A., 2003. Liquid chromatography with atmospheric pressure chemical ionization

and electrospray ionization mass spectrometry of flavonoids with triple-quadrupole and ion-trap instruments. J. Chromatogr. A 984, 45–58.

De Rijke, E., Zappey, H., Ariese, F., Gooijer, C., 2004. Flavonoids in Leguminosae: analysis of extracts of *T. pratense* L., *T. dubium* L., *T. repens* L., and *L. corniculatus* L. leaves using liquid chromatography with UV, mass spectrometric and fluorescence detection. Anal. Bioanal. Chem. 378, 995–1006.

Deavours, B.E., Liu, C.-J., Naoumkina, M., Tang, Y., Farag, M.A., Sumner, L.W., Noel, J.P., Dixon, R.A., 2006. Functional analysis of members of the isoflavone and isoflavanone O-methyltransferase enzyme families from the model legume *Medicago truncatula*. Plant Mol. Biol. 62, 715–733.

Dixon, R.A., 1999. Isoflavonoids: biochemistry, molecular biology, and biological functions. In: Barton, D., Nakanishi, K., Meth-Cohn, O. (Eds.), Comprehensive Natural Product Chemistry, vol. 1. Elsevier, New York, pp. 773–823.

Dixon, R.A., Sumner, L.W., 2003. Legume natural products. Understanding and manipulating complex pathways for human and animal health. Plant Physiol. 131, 878–885.

Edwards, R., Triller, S.A., Parry, A.D., 1997. The effect of plant age and nodulation on the isoflavonoid content of red clover (*Trifolium pratense*). J. Plant Physiol. 150, 603–610.

Gould, A.R., 1987. Staining and nuclear cytology of cultured cells. In: Vasil, I.K. (Ed.), Cell Culture and Somatic Cell Genetics of Plants, vol. 1. Academic Press, New York, pp. 698–710.

Halket, J.M., Pryzborowska, A., Stein, S.E., Mallard, G., Down, S., Chalmers, R.A., 1999. Deconvolution gas chromatography/mass spectrometry of urinary organic acids-potential for pattern recognition and automated identification of metabolic disorders. Rapid Commun. Mass Spec. 13, 279–284.

Harborne, J.B., 1994. For the content of "Flavonoids". In: Buckingham, J. (Ed.), Dictionary of Natural Products. Chapman and Hall, New York, pp. 449–468, and 673–700.

Hartwig, U.A., Maxwell, C.A., Joseph, C.M., Phillips, D.A., 1990. Chrysoeriol and luteolin released from alfalfa seeds induce nod genes in *Rhizobium meliloti*. Plant Physiol. 92, 116–122.

He, X.G., Lin, L.Z., Lian, L.Z., 1996. Analysis of flavonoids from red clover by liquid chromatography–electrospray mass spectrometry. J. Chromatogr. A 755, 127–132.

Huhman, D.V., Sumner, L.W., 2002. Metabolic profiling of saponins in *Medicago sativa* and *Medicago truncatula* using HPLC coupled to an electrospray ion-trap mass spectrometer. Phytochemistry 59, 347–360.

Jalal, M.A.F., Collin, H.A., 1977. Polyphenols of mature plant, seedling and tissue cultures of *Theobroma cacao*. Phytochemistry 16, 1377–1380.

Kamel, M.S., 2003. Flavone *C*-glycosides from *Lupinus hartwegii*. Phytochemistry 63, 449–452.

Kessmann, H., Edwards, R., Geno, P., Dixon, R.A., 1990. Stress responses in alfalfa (*Medicago sativa* L.) constitutive and elicitor-induced accumulation of isoflavonoid conjugates in cell suspension culture. Plant Physiol. 94, 227–232.

Klejdus, B., Vitamvásová-Štěrbová, D., Kubáň, V., 2001. Identification of isoflavone conjugates in red clover (*Trifolium pratense*) by liquid chromatography–mass spectrometry after two-dimensional solid-phase extraction. Anal. Chim. Acta 450, 81–97.

Klejdus, B., Sterbova, D., Stratil, P., Kuban, V., 2003. Identification and characterization of isoflavonoids in red clover using HPLC–PDA–MS. Chim. Listy 97, 530–539.

Latunde-Dada, A.O., Cabello-Hurtado, F., Czittrich, N., Didierjean, L., Schopfer, C., Hertkorn, N., Werck-Reichhart, D., Ebel, J., 2001. Flavonoid 6-hydroxylase from soybean (*Glycine max* L.), a novel plant P-450 monooxygenase. J. Biol. Chem. 276, 1688–1695.

Lin, L.Z., He, X.G., Lindenmaier, M., Yang, J., Cleary, M., Qiu, S.X., Cordell, G.A., 2000. LC–ESI–MS study of the flavonoid glycoside malonates of red clover (*Trifolium pratense*). J. Agric. Food Chem. 48, 354–365.

Mabry, T.J., Markham, K.R., Thomas, M.B., 1970. The Systematic Identification of Flavonoids. Springer-Verlag, New York.

Niessen, W.M.A., Tinke, A.P., 1995. Liquid chromatography–mass spectrometry. General principles and instrumentation. J. Chromatogr. A 703, 37–57.

Rabaneda, F.S., Jauregiu, O., Casals, I., Andres, C.A., Pulido, M.I., Raventos, R.M., 2003. Liquid chromatographic/electrospray ionization tandem mass spectrometric study of the phenolic composition of cocoa (*Theobroma cacao*). J. Mass Spectrom. 38, 35–42.

Rice-Evans, C.A., Miller, N.J., Paganga, G., 1997. Antioxidant properties of phenolic compounds. Trends Plant Sci. 2, 152–159.

Tiller, S.A., Party, A.D., Edwards, R., 1994. Changes in the accumulation of flavonoids and isoflavonoids conjugates associated with plant age and nodulation in alfalfa. Plant Physiol. 91, 27–36.

Wu, Q., Wang, M., Simon, J.E., 2003. Determination of isoflavones in red clover and related species by high-performance liquid chromatography combined with ultraviolet and mass spectrometric detection. J. Chromatogr. A 1016, 195–209.